

Aggregation Properties and Mixing Behavior of Hydrocarbon, Fluorocarbon, and Hybrid Hydrocarbon–Fluorocarbon Cationic Dimeric Surfactants

Reiko Oda,^{*,†} Ivan Huc,^{*,†} Dganit Danino,[‡] and Yashayahu Talmon[‡]

Institut Européen de Chimie et Biologie, Av. Pey Berland, 33402 Talence Cedex, France, and Department of Chemical Engineering, Technion–Israel Institute of Technology, Haifa 32000, Israel

Received June 8, 2000. In Final Form: September 14, 2000

The synthesis, phase behavior, and mixing properties of cationic dimeric (gemini) surfactants having one or two perfluoroalkyl chains is described and compared to that of analogue hydrocarbon surfactants. The combination of the dimeric character of the amphiphiles with the high hydrophobicity of the fluorocarbon chains leads to very low critical micelle concentration values and unusually low characteristic times of exchange between surfactants in the bulk solution and surfactants in the aggregate. This results in slow exchange on the NMR time scale, which allows a practical study of micellization and comicellization by NMR. With respect to the morphology of the aggregates, the fluorocarbon amphiphiles do not simply behave as more hydrophobic amphiphiles. Instead, they assemble into various structures including very stable unilamellar and multilamellar vesicles not seen in their hydrocarbon analogues. The hybrid hydrocarbon–fluorocarbon dimeric surfactant exhibits features of both families. In particular it mixes with either hydrocarbon or fluorocarbon surfactants, whereas the latter two undergo a macroscopic phase separation.

Introduction

Analogous to hydrocarbon amphiphiles, fluorocarbon amphiphiles self-assemble into various types of aggregates. They have attracted special interest because of several characteristics specific to fluorocarbons. Fluorine atoms have a low polarizability, and the volume of the hydrophobic fluorocarbon chain is about 1.5 times that of hydrocarbons.¹ Consequently, fluorinated chains are more hydrophobic, and fluorinated surfactants show much lower critical micellar concentration² (cmc) and higher surface activity compared to their hydrogenated counterparts.³

A unique characteristic of fluorocarbon chains is their simultaneous hydrophobic and lipophobic nature. Thus, fluorinated amphiphiles exhibit limited miscibility with hydrocarbon amphiphiles⁴ or organic solvents.⁵ One can observe macroscopic phase separation of hydrocarbon amphiphiles and fluorocarbon amphiphiles into different aggregates or microscopic phase separation within the same aggregates. This peculiar mixing behavior naturally stimulated interest in “hybrid” amphiphiles, bearing one hydrocarbon and one fluorocarbon chain. Kunitake et al. have combined fluorocarbon and hydrocarbon chains in various double- and triple-chain amphiphiles which all

form bilayers in aqueous solutions.⁶ They have shown that while 100% fluorocarbon amphiphiles are poorly miscible with 100% hydrocarbon amphiphiles, miscibility can be controlled using hybrid amphiphiles.

Recently interest has grown in “exotic” surfactant molecules such as dimeric (or “gemini”) surfactants⁷ due to the unusual morphologies and physical properties of their aggregates in solution.⁸ They are comprised of two conventional single-chain surfactant units connected at their headgroups by a spacer of variable length, rigidity, and polarity. Dimeric surfactants bearing cationic, anionic, and neutral headgroups have been reported. Bis(quaternary ammonium) bromides having the structure $C_3H_2\text{-}\alpha,\omega\text{-}(Me_2N^+C_mH_{2m+1}Br^-)_2$ referred to as $m\text{-}s\text{-}m$ are among the most studied dimeric surfactants. The effects of spacer length s ,⁹ of added salt,¹⁰ and of the nature of the counterions¹¹ on the morphology and the physical properties of self-assemblies have been investigated. Recently, we reported the synthesis and phase behavior of a series of dissymmetric gemini surfactants of the type $C_2H_4\text{-}\alpha,\omega\text{-}\{Me_2N^+C_nH_{2n+1}Br^-\}\text{-}\{Me_2N^+C_mH_{2m+1}Br^-\}$. Those compounds, referred to as $n\text{-}2\text{-}m$, have the same headgroups with a spacer of two carbons ($s = 2$) but have hydrocarbon chains of various length (Scheme 1).¹² It was

* To whom correspondence should be addressed: e-mail, reiko.oda@iecb-polytechnique.u-bordeaux.fr and ivan.huc@iecb-polytechnique.u-bordeaux.fr.

(1) Mukerjee, P.; Mysels, K. J. *ACS Symp. Ser.* **1975**, *9*, 239.

(2) (a) Mukerjee, P.; Mysels, K. J. *Critical micelle concentrations of aqueous surfactant systems*, NSRDS–NBS-36, U.S. Government Printing office, Washington, D.C., **1971**. (b) Shinoda, K.; Hato, M.; Hatashi, T. *J. Phys. Chem.* **1972**, *76*, 909.

(3) Kuniieda, H.; Shinoda, K. *J. Phys. Chem.* **1976**, *80*, 2468.

(4) (a) Mukerjee, P.; Yang, A. Y. S. *J. Phys. Chem.* **1976**, *80*, 13881; (b) Elbert, R.; Folda, T.; Ringsdorf, H. *J. Am. Chem. Soc.* **1984**, *106*, 7687. (c) Tamori, K.; Ishikawa, A.; Kihara, K.; Ishii, Y.; Esumi, K. *Colloids and Surfaces* **1992**, *67*, 1.

(5) (a) Ishikawa, Y.; Kuwahara, H.; Kunitake, T. *Chem. Lett.* **1989**, 1737. (b) Ishikawa, Y.; Kuwahara, H.; Kunitake, T. *J. Am. Chem. Soc.* **1989**, *111*, 8530. (c) Kuwahara, H.; Hamada, M.; Ishikawa, Y.; Kunitake, T. *J. Am. Chem. Soc.* **1993**, *115*, 3002.

(6) (a) Kunitake, T.; Tawaki, S.; Nakashima, N. *Bull. Chem. Soc. Jpn* **1983**, *56*, 3235. (b) Kunitake, T.; Higashi, N. *J. Am. Chem. Soc.* **1985**, *107*, 692.

(7) (a) Menger, F. M.; Littau, C. A. *J. Am. Chem. Soc.* **1991**, *113*, 1451. (b) Zana, R.; Benrraou, M.; Rueff, R. *Langmuir* **1991**, *7*, 1072.

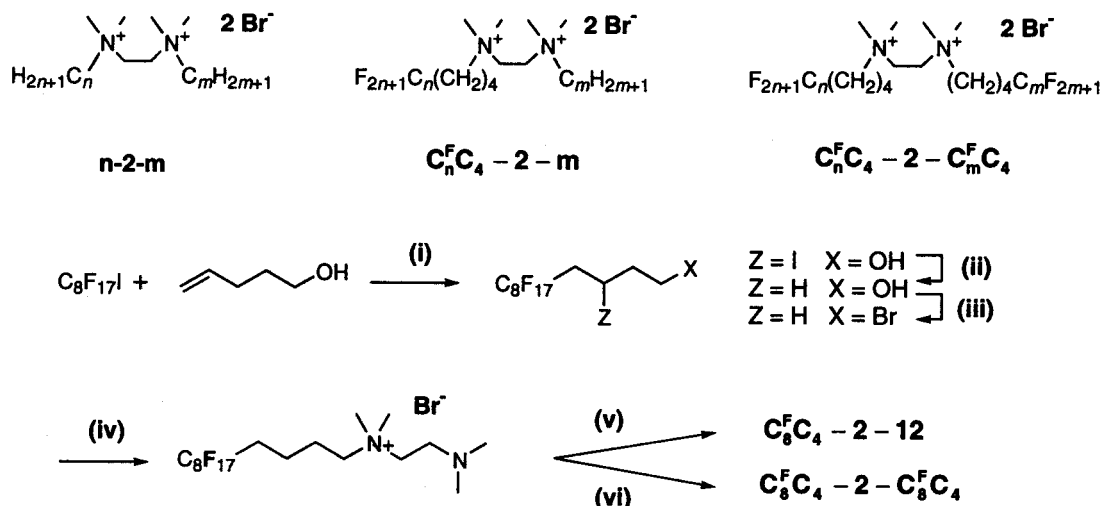
(8) For a review see: Rosen, M. J.; Tracy, D. J. *J. Surfactants Detergents* **1998**, *1*, 547.

(9) Danino, D.; Talmon, Y.; Zana, R. *Langmuir* **1995**, *11*, 1448.

(10) (a) Bühler, E.; Mendes, E.; Boltzenhagen, P.; Munch, J. P.; Zana, R.; Candau, S. J. *Langmuir* **1997**, *13*, 3096. (b) Knaebel, A.; Oda, R.; Mendes, E.; Candau, S. J. *Langmuir* **2000**, *16*, 2489.

(11) (a) Oda, R.; Huc, I.; Candau, S. J. *Ang. Chem. Int. Ed.* **1998**, *37*, 2689. (b) Oda, R.; Huc, I.; Schmutz, M.; Candau, S. J.; MacKintosh, F. C. *Nature* **1999**; (c) Bhattacharya, S.; De, Soma *Langmuir* **1999**, *15*, 3400.

(12) (a) Oda, R.; Huc, I.; Homo, J.-C.; Heinrich, B.; Schmutz, M.; Candau, S. J. *Langmuir* **1999**, *15*, 2384. (b) Oda, R.; Huc, I.; Candau, S. J. *Chem. Commun.* **1997**, 2105.

Scheme 1. Structure of the Hydrocarbon, Fluorocarbon, and Hybrid Hydrocarbon–Fluorocarbon Cationic Gemini Surfactants^a

^a Synthetic route followed for the preparation of $\text{C}_8^{\text{F}}\text{C}_4-2-\text{C}_8^{\text{F}}\text{C}_4$ and $\text{C}_8^{\text{F}}\text{C}_4-2-12$: (i) Cu^0 Cat., 120 °C, 2 h, 82%; (ii) Bu_3SnH , 80 °C, 2 h, 84%; (iii) $(\text{CH}_3\text{SO}_2)_2-\text{EtPr}_2\text{N}$, then LiBr -acetone, 78%; (iv) TMEDA 1 equiv, CH_3CN 40 °C, 24 h, 90%; (v) $\text{C}_{12}\text{H}_{25}\text{Br}$ 2 equiv, CH_3CN 80 °C, 2 days, 65%; (vi) $\text{C}_8\text{F}_{17}(\text{CH}_2)_4\text{Br}$ 1.2 equiv, CH_3CN 4 days, 60%.

noted that those gemini surfactants have a tendency to form elongated and stacked bilayer structures which differ fundamentally from the phases formed by their corresponding monomeric ammonium bromides.

In the present study we report the synthesis of fluorocarbon and hybrid hydrocarbon–fluorocarbon cationic gemini surfactants, their phase behavior, and their mixing behavior with their hydrogenated counterparts. The structures of the new fluorocarbon $\text{C}_8^{\text{F}}\text{C}_4-2-\text{C}_8^{\text{F}}\text{C}_4$ and hybrid $\text{C}_8^{\text{F}}\text{C}_4-2-12$ surfactants are depicted in Scheme 1. The techniques we applied are cryogenic transmission electron microscopy (cryo-TEM), ^1H and ^{19}F nuclear magnetic resonance (NMR), conductimetry, and light microscopy.

Experimental Section

Synthesis. (a) 5,5,6,6,7,7,8,8,9,9,10,10,11,11,12,12,12-Heptadecafluoro-3-iodo-1-dodecanol.¹³ Fine copper powder (283 mg, 4.5 mmol), 1-iodo-perfluorooctane (11.88 mL, 45 mmol), and 3-buten-1-ol (4.5 mL, 54 mmol) were mixed in a pressure tube and heated at 120 °C for 2 h with vigorous magnetic stirring. After cooling to room temperature, the solid residue was dissolved in warm chloroform and filtered warm. The filtrate was evaporated to dryness and then dissolved in hot *n*-hexane (250 mL). After the solution was allowed to stand at 7 °C, the crystallized product (20.7 g) was filtered off. The mother liquor was concentrated and allowed to stand at 7 °C to yield a further 2.2 g. Yield: 22.9 g (82%). 400 MHz ^1H NMR (CDCl_3 , TMS): δ 4.54 (m, 1H), 3.90 (m, 1H), 3.80 (m, 1H), 2.93 (m, 2H), 2.04 (m, 2H). ^{19}F NMR (CDCl_3 , CFCl_3): δ -81.71 (t, $J_3 = 9.3$ Hz, 3F), -112.45 (d, $J_2 = 270$ Hz, 1F), -115.12 (d, $J_2 = 270$ Hz, 1F), -122.49 (m, 2F), -122.83 (m, 4F), -123.64 (m, 2F), -124.53 (m, 2F), -127.04 (m, 2F). Anal. Found: C, 23.5; H, 1.2. Calcd for $\text{C}_{12}\text{H}_8\text{F}_{17}\text{O}$: C, 23.32; H, 1.30.

(b) 5,5,6,6,7,7,8,8,9,9,10,10,11,11,12,12,12-Heptadecafluoro-1-dodecanol.¹³ Heptadecafluoro-3-iodo-1-decanol (20.5 g, 33 mmol) and tributyltin hydride (10.6 mL, 40 mmol) were mixed in a pressure tube and heated at 80 °C for 2 h with vigorous magnetic stirring. After cooling to room temperature, the residue was dissolved in hot hexane and filtered hot. The product crystallized upon standing at 7 °C. It was collected by filtration and recrystallized once more from *n*-hexane (hot to 7 °C). Yield: 13.8 g (84%). 400 MHz ^1H NMR (CDCl_3 , TMS): δ 3.70 (broad m, 2 H), 2.11 (m, 2 H), 1.74–1.64 (m, 4H). ^{19}F NMR (CDCl_3 ,

CFCl_3): δ -81.73 (t, $J_3 = 9.2$ Hz, 3F), -115.38 (m, 2F), -122.67 (m, 2F), -122.87 (m, 4F), -123.67 (m, 2F), -124.46 (m, 2F), -127.04 (m, 2F). Anal. Found: C, 29.7; H, 1.9. Calcd for $\text{C}_{12}\text{H}_9\text{F}_{17}\text{O}$: C, 29.28; H, 1.84.

(c) 5,5,6,6,7,7,8,8,9,9,10,10,11,11,12,12,12-Heptadecafluoro-1-bromododecane. Heptadecafluoro-1-dodecanol (13.7 g 27.8 mmol) was dissolved in anhydrous THF (250 mL). The solution was cooled in an ice bath and methanesulfonic anhydride (7.27 g, 1.5 equiv) was added, followed by ethyldiisopropylamine (2 equiv freshly distilled from CaH_2). The mixture was stirred at 0 °C for 1 h and at room temperature for 2 h. It was then filtered, and the filtrate was evaporated. The residue was dissolved in acetone (100 mL). LiBr (8 equiv) was added, and the mixture was heated to reflux for 12 h. The acetone was evaporated, and the residue was partitioned between water and petroleum ether. The organic layer was washed twice with aqueous 0.5 M H_2SO_4 , dried (MgSO_4), filtered, and concentrated. It was then passed through a short pad of silica gel, eluting with *n*-hexane. Upon allowing the solution to stand at -18 °C, the product crystallized from *n*-hexane. Three crops were combined to yield 12 g (78%). NMR analysis showed that traces of the starting alcohol remained. 400 MHz ^1H NMR (CDCl_3 , TMS): δ 3.43 (t, $J = 6.5$ Hz, 2 H), 2.11 (m, 2 H), 1.96 (m, 2 H), 1.80 (m, 2 H). ^{19}F NMR (CDCl_3 , CFCl_3): δ -81.71 (t, $J_3 = 9.2$ Hz, 3F), -115.24 (m, 2F), -122.63 (m, 2F), -122.85 (m, 4F), -123.64 (m, 2F), -124.41 (m, 2F), -127.03 (m, 2F).

(d) Monoquaternization of Tetramethylethylenediamine with Heptadecafluoro-1-bromododecane. The alkyl bromide (4.6 mM) and tetramethylethylenediamine (715 μL , 1 equiv) were dissolved in CH_3CN and heated at 40 °C for 48 h. The solvent was evaporated (low vacuum is recommended to avoid foaming), and the residue was dried at 65 °C under vacuum (10^{-2} mbar). ^1H NMR (400 MHz) showed no trace of the starting material, and the product was used in the next step without further purification. ^1H NMR (CDCl_3 , TMS): δ 3.84 (t, $J = 5.6$ Hz, 2 H), 3.79 (m, 2 H), 3.47 (s, 6 H), 2.81 (t, $J = 5.2$ Hz, 2 H), 2.31 (s, 6 H), 2.29–2.17 (m, 2H), 1.92 (m, 2 H), 1.75 (m, 2H).

Synthesis of $\text{C}_8^{\text{F}}\text{C}_4-2-12$ and $\text{C}_8^{\text{F}}\text{C}_4-2-\text{C}_8^{\text{F}}\text{C}_4$. The monoquaternized tetramethylethylenediamine (4 mM) and the alkyl bromide (1.2 equiv of either 1-bromododecane or heptadecafluoro-1-bromododecane) in 15 mL of anhydrous CH_3CN were heated to 80 °C for 3 days. The mixture was evaporated to dryness. $\text{C}_8^{\text{F}}\text{C}_4-2-12$ was recrystallized three times from acetone/chloroform. ^1H NMR (97/3, $\text{CDCl}_3/\text{CD}_3\text{OD}$, TMS): δ 4.46 (s, 4 H), 3.68 (m, 2 H), 3.57 (m, 2 H), 3.37 (s, 6 H), 3.33 (s, 6 H), 2.22 (m, 2 H), 1.93 (m, 2 H), 1.75 (m, 4H), 1.37 (m, 2 H), 1.24 (m, 16 H), 0.86 (t, $J = 6.9$ Hz, 3 H). Anal. Found: C, 39.1; H, 5.3; N, 2.9; Br, 17.1. Calcd for $\text{C}_{30}\text{H}_{49}\text{F}_{17}\text{Br}_2\text{N}_2$: C, 39.14; H, 5.37; N, 3.04; Br, 17.36.

(13) Kotora, M.; Hájek, M.; Ameduri, B.; Boutevin, B. *J. Fluorine Chem.* **1994**, *68*, 49.

$C_8^F C_4-2-C_8^F C_4$ was dissolved in a warm mixture of CH_2Cl_2 and MeOH. Heptane was added and CH_2Cl_2 and MeOH were distilled. The product was filtered from boiling heptane. 1H NMR (90/10, $CDCl_3/CD_3OD$, TMS): δ 4.30 (s, 4 H), 3.56 (m, 4 H), 3.27 (s, 12 H), 2.20 (m, 4 H), 1.88 (m, 4 H), 1.68 (m, 4 H). Anal. Found: C, 29.4; H, 2.5; N, 2.1; Br, 13.1. Calcd for $C_{30}H_{32}F_{34}Br_2N_2$: C, 29.38; H, 2.63; N, 2.28; Br, 13.03.

Sample Preparations. Samples were prepared by directly mixing the surfactants in Millipore deionized water (18.2 M Ω) in small bottles. After thorough mixing at 60 °C and sonication, they were left at 25 °C for more than 24 h to reach equilibrium. Due to the difficulty in knowing whether the solution has reached equilibrium, observations were performed with samples a few hours after being prepared, as well as samples which were 3 months old. No noticeable differences were observed.

Some of the macroscopic phase separations were very slow and were left for up to 10 days. Special care was taken to avoid partial remixing of separated phases while drawing samples of either lower or upper phases. Specifically, needles were inserted at the top and the bottom of the solution through an airtight cap prior to phase separation. These samples were observed by light microscopy and cryo-TEM.

Electrical Conductivity. The electrical conductivity of the surfactant solutions was measured as a function of concentration with a conductivity meter, model CD810 (Tacussel électronique). A fraction of a solution about 5 to 10 times more concentrated than the estimated cmc of the surfactant was added to 20 mL of deionized water, and the conductivity was registered as it reached an equilibrium value. The time to reach equilibrium varied significantly from one system to the next. For $C_8^F C_4-2-C_8^F C_4$, which forms a very stable vesicular solution, up to 15 h was required to reach equilibrium. The cell was covered to avoid evaporation. The cmc value was obtained as the break in the conductivity, κ ($\mu S \cdot cm^{-1}$), vs concentration (C) curve, as well as the break in equivalent conductivity, Λ ($mS \cdot cm^2 \cdot mol^{-1}$), vs the square root of concentration ($C^{1/2}$).

Cryo-TEM. Vitrified specimens were prepared for direct imaging cryo-TEM in a controlled environment vitrification system (CEVS), at 25 °C and a relative humidity of 100%.¹⁴ A droplet of the solution to be investigated was deposited onto a 200 mesh copper grid coated with a perforated carbon film and blotted with filter paper to form a thin film of solution, about 200 nm thick in the middle of the holes. The blotted specimens were plunged into liquid ethane at its freezing point to ensure the vitrification and stored in liquid nitrogen. It has to be noted that large aggregates such as vesicles having diameters greater than the thickness of the sample film are flattened. In addition, large objects may be removed by blotting. The grids were then transferred to an Oxford CT-3500 cryo holder and examined in a Philips CM120 microscope, operated at 120 kV at temperatures below -178 °C. Images were recorded digitally by a Gatan 791 MultiScan CCD camera with the DigitalMicrograph software package. The Adobe Photoshop package was used for image processing.

Phase Contrast Light Microscope. Light microscopy observations were made with an Olympus CX40 microscope using a 40 times objective lens (numerical aperture 0.65) and phase contrast optics. The images were processed using a Sony DKC-CM30 digital camera.

NMR spectra were recorded on an Ultrashield Bruker Avance 400 MHz spectrometer. A spin-echo pulse sequence was used for ^{19}F NMR.

Results

To perform a comparative study between hydrocarbon and fluorocarbon surfactants, we decided to investigate fluorinated compounds closely resembling their $n-2-m$ hydrocarbon analogues that would be both stable and easy to prepare. The $-CF_2-N^+$ moiety does not form under mild conditions, $-CF_2-CH_2-N^+$ tends to hydrolyze, and $-CF_2-(CH_2)_2-N^+$ is prone to β elimination. Thus, a

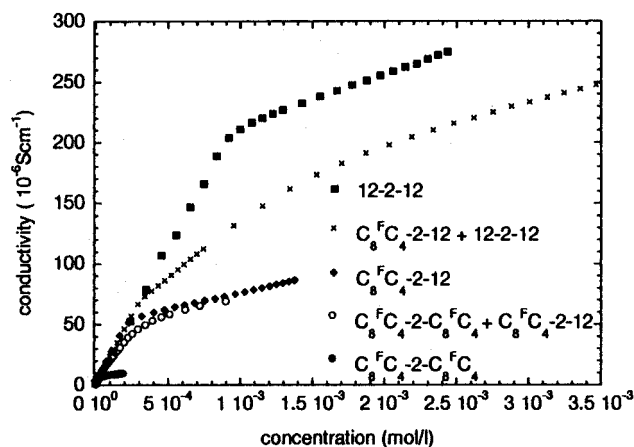


Figure 1. Conductivity, κ , vs concentration curves of solutions of 12-2-12, $C_8^F C_4-2-12$, and $C_8^F C_4-2-C_8^F C_4$ and of equimolar mixtures of $C_8^F C_4-2-12$ and 12-2-12 and of $C_8^F C_4-2-12$ and $C_8^F C_4-2-C_8^F C_4$. For the mixed solutions, the concentration is the total concentration of both surfactants. The conductivity increases linearly below the cmc, and the slopes are identical for all the solutions. The two mixed solutions show only one break.

hydrocarbon spacer at least three carbon units long between the perfluoroalkyl chain and the ammonium group is necessary. We used a straightforward synthetic scheme which introduces a four-carbon spacer $-(CH_2)_4-$ (Scheme 1). That way, the synthesis requires only inexpensive hydrocarbon and perfluorocarbon alkyl halide precursors, all having an even number of carbons. Thus, the synthesis of $C_8^F C_4-2-C_8^F C_4$ and $C_8^F C_4-2-12$ was performed in two steps from tetramethylethylenediamine (TMEDA), bromododecane, and 5,5,6,6,7,7,8,8,9,9,10,10,11,11,12,12,12-heptafluoro-1-bromododecane. As described in the Experimental Section, this latter substance was prepared using a modified version of protocols reported for shorter fluorocarbon analogues.¹³

The concentration-dependent aggregation properties of 12-2-12, $C_8^F C_4-2-C_8^F C_4$, and $C_8^F C_4-2-12$, all bearing two 12 carbon long hydrophobic chains, were studied using conductivity, 1H and ^{19}F NMR, and light and electron microscopies. In the following, the phase behavior is described at 25 °C, unless indicated otherwise.

Aggregation Properties of Hydrogenated, Fluorinated, and Hybrid Hydrogenated-Fluorinated Gemini Surfactants. (a) Hydrocarbon 12-2-12. The aggregation behavior of the hydrocarbon surfactant 12-2-12 follows the trend described for other $n-2-m$ surfactants¹² and has, to a large extent, been reported in the literature. For the purpose of the present comparative study, essential characteristics are summarized below. The cmc of 12-2-12 was determined by conductivity to be 0.95 mM (Figure 1). Below this concentration the 1H NMR spectrum of a D_2O solution is sharp and concentration independent. Above 0.95 mM, the NMR signals shift and broaden with concentration, as they are average signals of surfactant molecules in the bulk and in the micelles (data not shown).¹⁵ As the concentration is increased, elongated cylindrical micelles (threadlike micelles) are observed by cryo-TEM.¹⁶ Beyond 24 mM for solutions in H_2O and 19 mM in D_2O (the overlap concentration C^*), these micelles are entangled and the viscosity of the solution rapidly increases with concentra-

(15) Huc, I.; Oda, R. *Chem. Commun.* **1999**, 2025.

(16) (a) Zana, R.; Talmon, Y. *Nature* **1993**, *362*, 228. (b) Bernheim-Groszasser, A.; Zana, R.; Talmon, Y. *J. Phys. Chem. B* **2000**, *17*, 4005.

(14) Bellare, J. R.; Davis, H. T.; Scriven, L. E.; Talmon, Y. J. *Electron Microsc. Technol.* **1988**, *10*, 87.

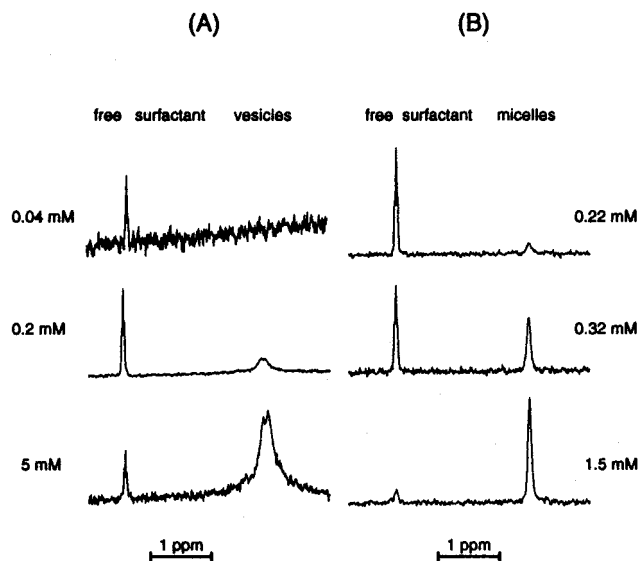


Figure 2. Part of the 400 MHz ^{19}F NMR spectra of $\text{C}_8^{\text{F}}\text{C}_4-2-\text{C}_8^{\text{F}}\text{C}_4$ (A) and $\text{C}_8^{\text{F}}\text{C}_4-2-12$ (B) at various concentrations in 9:1 $\text{H}_2\text{O}/\text{D}_2\text{O}$ (25 °C). The region contains the signals of the terminal $-\text{CF}_3$ groups in the bulk and in the aggregates.

tion.^{17,18} At these concentrations, micelle branching is observed.^{16,18} At about 150 mM, stacked bilayer membranes appear as is the case for other $n-2-m$ hydrocarbon gemini surfactants,¹² and the solution becomes birefringent. These bilayer aggregates tend to have elongated shapes (ribbon-like structures). At higher temperatures, micelles are shorter, and C^* and the appearance of the stacked bilayer membranes are shifted toward higher concentrations.

(b) Fluorocarbon Surfactant $\text{C}_8^{\text{F}}\text{C}_4-2-\text{C}_8^{\text{F}}\text{C}_4$. The aggregation behavior of the fluorinated surfactant $\text{C}_8^{\text{F}}\text{C}_4-2-\text{C}_8^{\text{F}}\text{C}_4$ differs strongly from that of 12-2-12. Due to the higher hydrophobicity of the fluorocarbon chains, its cmc is 2 orders of magnitude lower (28 μM by conductimetry, Figure 1). Below the cmc, the ^1H and ^{19}F NMR signals of D_2O (^1H NMR) or 9/1 $\text{H}_2\text{O}/\text{D}_2\text{O}$ (^{19}F NMR) solutions are sharp. However above the cmc, the NMR signals of the surfactants in the bulk do not shift and new signals corresponding to the aggregate appear at higher fields (Figure 2A). This indicates slow exchange of surfactant molecules between the bulk phase and the aggregate on the NMR time scale, corresponding to an unusually low characteristic time of exchange for a cationic amphiphile.¹⁵ The signals in the aggregate are shifted 1–2 ppm upfield from those of the free surfactant, which is consistent with a decrease in polarity from the bulk water to the fluorocarbon environment. When compared with an internal $\text{CF}_3\text{CH}_2\text{OH}$ standard, the intensity of the signals of the free surfactant increases linearly with concentration up to the cmc, and levels off above the cmc. The break between these two curves allows a cmc of 30 μM to be estimated. This is in agreement with the value recorded by conductimetry. Above this value, the intensity of the signals assigned to the aggregate increases, but the signals are very broad and integration becomes inaccurate.

Several factors suggest that the aggregates formed by $\text{C}_8^{\text{F}}\text{C}_4-2-\text{C}_8^{\text{F}}\text{C}_4$ above its cmc are not micellar: (i) The slope of conductivity vs concentration just above the cmc

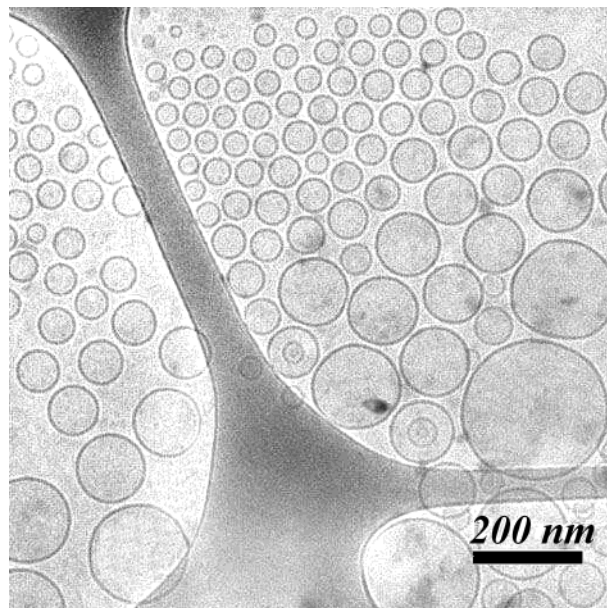


Figure 3. Cryo-TEM image of a 4 mM solution of $\text{C}_8^{\text{F}}\text{C}_4-2-\text{C}_8^{\text{F}}\text{C}_4$ at 25 °C. Small unilamellar vesicles are observed.

is indicative of the nature of aggregation. For $n-2-m$ gemini, this slope above the cmc is $\sim 10^4 \mu\text{S}\cdot\text{cm}^{-1}\cdot\text{mol}^{-1}$ for bilayer-forming gemini surfactants, while for micelle-forming gemini surfactants it is $\sim 5 \times 10^4 \mu\text{S}\cdot\text{cm}^{-1}\cdot\text{mol}^{-1}$.¹⁹ $\text{C}_8^{\text{F}}\text{C}_4-2-\text{C}_8^{\text{F}}\text{C}_4$ shows a slope very close to that of bilayer-forming gemini such as 16-2-18. (ii) The signals assigned to the aggregate are very broad at any concentration suggesting strong solid interactions in the aggregate (Figure 2A vs Figure 2B). (iii) Dilute solutions of $\text{C}_8^{\text{F}}\text{C}_4-2-\text{C}_8^{\text{F}}\text{C}_4$ are fluid and slightly opaque.

These observations are consistent with the formation of bilayers above the cmc. Indeed, direct observation of a 4 mM solution by cryo-TEM revealed the presence of spherical mostly unilamellar vesicles, 15–200 nm in diameter (Figure 3). These vesicles form readily by dispersing $\text{C}_8^{\text{F}}\text{C}_4-2-\text{C}_8^{\text{F}}\text{C}_4$ in water at room temperature.²⁰ They are very stable, and no transition is observed upon heating the solution up to 70 °C. Upon aging, some graduation in opacity of the solution is observed indicating that the vesicles have a higher density than water. Above 15 mM a macroscopic phase separation is observed, and a viscous and opaque phase appears at the bottom of the sample. This phase is slightly birefringent, consisting of multilamellar vesicles with diameters up to several micrometers, according to phase-contrast microscopy (Figure 4). The volume ratio of the bottom phase increases with concentration, and above 150 mM, it spans the entire sample.

(c) Hybrid Hydrocarbon–Fluorocarbon Surfactant $\text{C}_8^{\text{F}}\text{C}_4-2-12$. The aggregation properties of the hybrid surfactant $\text{C}_8^{\text{F}}\text{C}_4-2-12$ show features of both its hydrocarbon analogue, 12-2-12, and its fluorocarbon analogue, $\text{C}_8^{\text{F}}\text{C}_4-2-\text{C}_8^{\text{F}}\text{C}_4$. The cmc was determined by conductivity to have an intermediate value of 0.2 mM (Figure 1). As for $\text{C}_8^{\text{F}}\text{C}_4-2-\text{C}_8^{\text{F}}\text{C}_4$, the characteristic time of exchange of $\text{C}_8^{\text{F}}\text{C}_4-2-12$ between the bulk phase and the aggregate is low enough that two sets of signals appear

(17) (a) Kern, F.; Lequeux, F.; Zana, R.; Candau, S. J. *Langmuir* **1994**, *10*, 1714. (b) MacKintosh, F. C.; Safran, S. A.; Pincus, P. A. *Europhys. Lett.* **1990**, *12*, 697.

(18) Oda, R.; Panizza, P.; Schmutz, M.; Lequeux, F. *Langmuir* **1997**, *13*, 6407.

(19) Oda, R. unpublished results.

(20) By comparison, long-chain $n-2-m$ hydrocarbon gemini have elevated Krafft temperatures, and dissolve upon heating to give metastable dispersions. See: Zhao, J.; Christian, S. D.; Fung, B. M. J. *Phys. Chem.* **1998**, *102*, 7613.

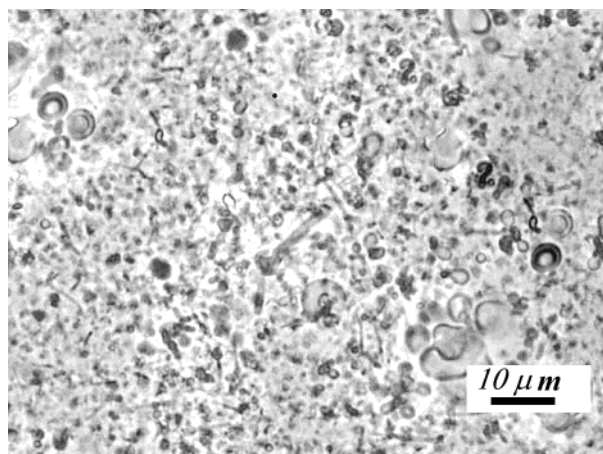


Figure 4. Phase contrast light microscope image of the lower phase of a $C_8^F C_4-2-C_8^F C_4$ solution at 40 mM.

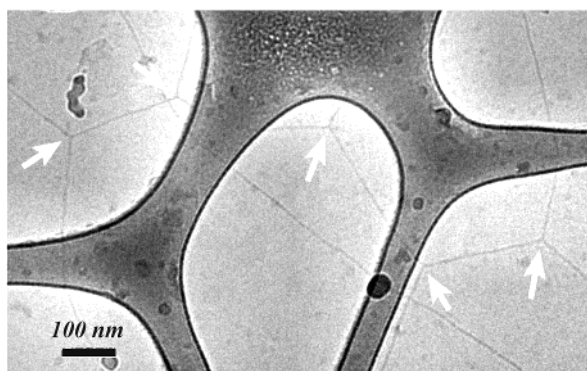


Figure 5. Cryo-TEM image of a $C_8^F C_4-2-12$ solution at 3.6 mM. Very long and branched micelles are observed. White arrows show 3-fold junctions.

on 1H and ^{19}F NMR spectra above the cmc, one corresponding to the free surfactant, and the other corresponding to the aggregate (Figure 2B).^{15,21} The cmc value as determined by NMR (0.2 mM) matches that measured by conductimetry.

Just above the cmc, the solution remains transparent and fluid. NMR signals assigned to the aggregates are only slightly broadened by the exchange, and the slope of conductivity vs concentration is $\sim 5 \times 10^4 \mu S \cdot cm^{-1} \cdot mol^{-1}$, suggesting that micelles are formed.

With the concentration increased further, the solution remains transparent but becomes highly viscoelastic (presence of recoil movement of bubbles captured in the solution) at about 2 mM. By analogy with the fully hydrogenated systems, this suggests the presence of long and entangled cylindrical micelles. The ^{19}F NMR signals assigned to the aggregate remain relatively sharp. Cryo-TEM images of a 3.6 mM solution show mostly branched cylindrical micelles coexisting with some unilamellar vesicles. The cylindrical micelles are very long ($> 1 \mu m$) and often form saturated networks, with the distance between branching points on the order of several micrometers²² (Figure 5). The vesicle diameters vary from tens to hundreds of nanometers. Upon further concentration, the solution becomes fluid again at around 5 mM

(21) A more thorough investigation of the exchange rates of various dimeric ammonium bromides using 2D exchange spectroscopy is now in progress.

(22) Such behavior of apparently rigid micelles forming branches of 120 degrees was also observed in the Habon G system (Danino et al. *Langmuir*, submitted).

and the ^{19}F NMR signals broaden significantly. The solution is then very slightly translucent. Cryo-TEM images at this concentration show the coexistence of polydisperse unilamellar vesicles, long and branched threadlike micelles, and suspended ribbons and bilayers (Figure 6A). The transformation of threadlike micelles into bilayers through ribbons of increasing width is observed (Figure 6B). It is also seen that threadlike micelles or narrow ribbons are connected to unilamellar vesicles (Figure 6C). Some small broken vesicles and flat bilayers are also seen (Figure 6D). These fluid solutions become viscous upon heating indicating the transition from bilayers to threadlike micelles.²³

Beyond 10 mM, macroscopic phase separation is observed. The upper phase is fluid and slightly opaque. Cryo-TEM and light microscopy images reveal that it consists of threadlike micelles, ribbons, and suspended bilayers coexisting essentially with small unilamellar vesicles (not shown). The lower phase is more opaque, viscous, and slightly birefringent. It consists mainly of packed lamellae and highly polydisperse multilamellar vesicles up to a few micrometers in diameter. Some threadlike micelles are also present, probably indicating incomplete phase separation (not shown). Beyond 50 mM, the lower phase spans the entire sample.

Mixing Behavior. In the following, the mixing behavior of 12-2-12, $C_8^F C_4-2-12$, and $C_8^F C_4-2-C_8^F C_4$ within their aggregates is reported. In all cases equimolar mixed solutions of two different surfactants were prepared. The phases formed were studied at various concentrations and temperatures using conductivity measurements, NMR, cryo-TEM, and light microscopy.

(a) Mixing Behavior of Hydrocarbon 12-2-12 and Fluorocarbon $C_8^F C_4-2-C_8^F C_4$. The conductivity vs concentration curve shows two breaks when the concentration of each surfactant reaches $22 \mu M$ and 0.8 mM (Figure 7), indicating that two kinds of aggregates are formed. These values are slightly lower, but very close to the cmc of $C_8^F C_4-2-C_8^F C_4$ ($28 \mu M$) and of 12-2-12 (0.95 mM), which suggests almost total phase separation between aggregates of the two surfactants. At a concentration of 2 mM of each surfactant the ^{19}F NMR spectrum is identical to that of $C_8^F C_4-2-C_8^F C_4$ alone at the same concentration. Thus, if any hydrocarbon surfactant is incorporated in the aggregates of $C_8^F C_4-2-C_8^F C_4$, it does not cause any shift of the signals despite the high sensitivity of ^{19}F nuclei.

Two phases are macroscopically separated above 5 mM of each surfactant and up to 320 mM. The phase behavior of the lower and upper layers closely resembles those of independent solutions of $C_8^F C_4-2-C_8^F C_4$ and 12-2-12, respectively. Thus, the upper phase is fluid and transparent and becomes viscoelastic as concentration is increased. The viscosity decreases upon heating. Cryo-TEM images of the upper phase of a 40 mM solution²⁴ show entangled threadlike micelles (Figure 8A) confirming the strong analogy to 12-2-12 solutions. The lower phase is opaque and not affected by heating. Cryo-TEM observation of a 40 mM solution²⁴ shows that this phase contains unilamellar vesicles, ranging from 50 to 500 nm, and multilamellar vesicles (Figure 8B), similar to that formed by $C_8^F C_4-2-C_8^F C_4$ alone.

(b) Mixing Behavior of Hydrocarbon 12-2-12 and Hybrid Hydrocarbon-Fluorocarbon

(23) Salkar, R. A.; Hassan, P. A.; Samant, S. D.; Valaulikar, B. S.; Kumar, V. V.; Kern, F.; Candau, S. J.; Manohar, C. *Chem. Commun.* **1996**, 1223.

(24) Concentration of each surfactant in the entire sample. The concentration of each surfactant is expected to be higher in one phase-separated layer, and lower in the other layer.

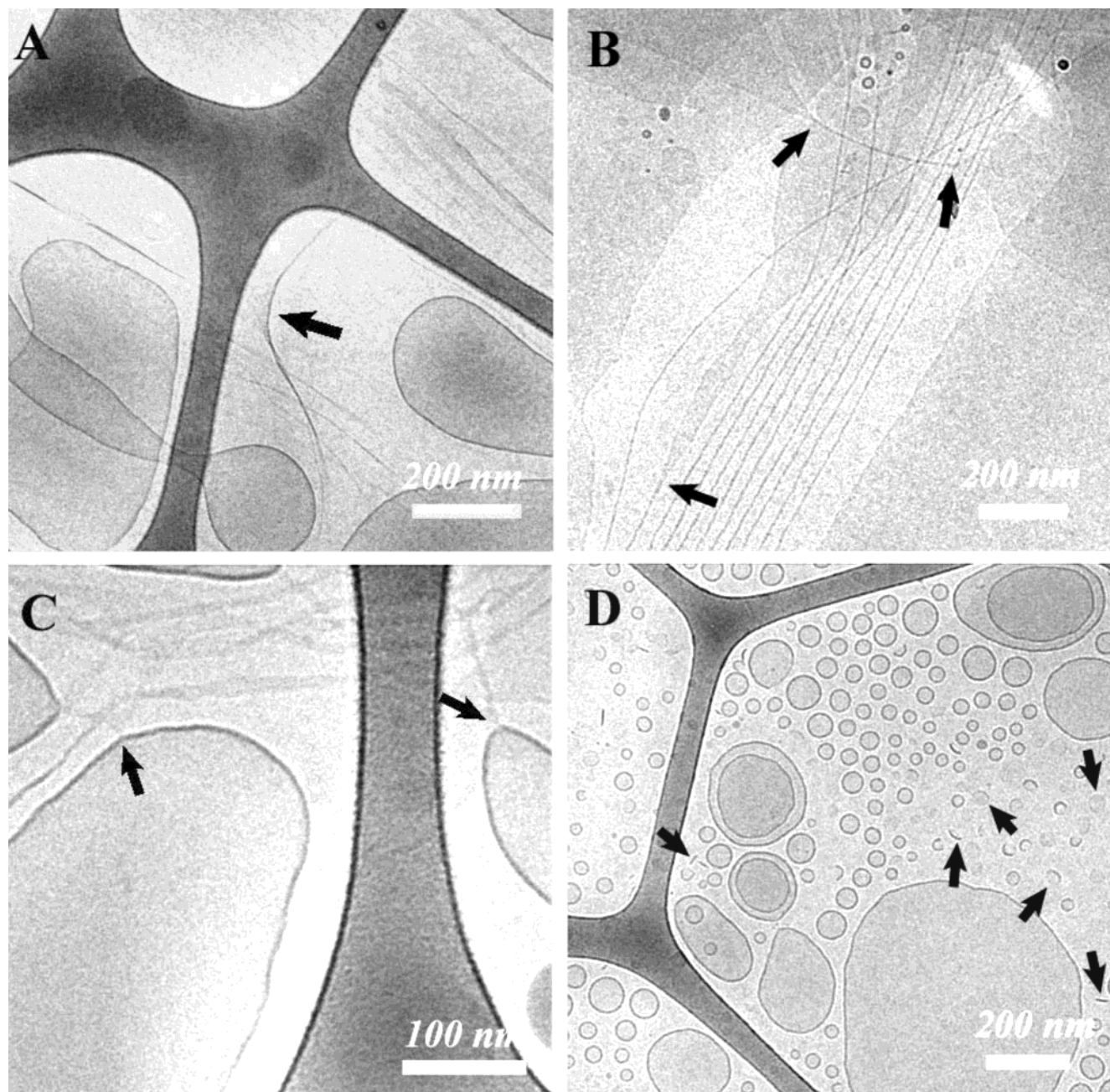


Figure 6. Cryo-TEM images of $C_8^F C_4-2-12$ solution at 5.6 mM (A). Very long micelles, bilayers, and vesicles coexist. Threadlike micelles transforming to bilayers (black arrows) (B) and to vesicles (black arrows) (C) can be seen. Some bilayer disks are also seen (D).

$C_8^F C_4-2-C_8^F C_4$. The conductivity vs concentration curve (Figure 1) of this mixture shows only one break at $[12-2-12] = [C_8^F C_4-2-12] = 0.13$ mM. This is substantially less than the cmc's of either surfactant (0.95 and 0.2 mM, respectively), which indicates comicellization of the two surfactants. The conductimetry data can be fitted using the regular solution theory (see Appendix),²⁵ yielding an interaction parameter $\beta = -1.24 \pm 0.30$. Such a negative value reflects an attractive interaction between 12-2-12 and $C_8^F C_4-2-12$. Thus, the surfactant distribution in the aggregates deviates from a statistical distribution expected for perfect mixing ($\beta = 0$).

Slow exchange between $C_8^F C_4-2-12$ in the bulk and in the micelles allows the tracing of comicellization by ^{19}F NMR (Figure 9B). Thus, when 12-2-12 and $C_8^F C_4-2-12$ are mixed in different proportions, it can clearly be seen that the hybrid hydrocarbon-fluorocarbon surfactant exists predominantly in the micellar state at concentrations close to and even below its cmc (Figure 9B). $C_8^F C_4-2-12$ thus remains in micelles consisting for the most part of 12-2-12 molecules. As the proportion of 12-2-12 in the micelles increases, the fluorocarbon chain of $C_8^F C_4-2-12$ is less shielded than in micelles of pure $C_8^F C_4-2-12$, and the ^{19}F NMR signals shift as much as 0.6 ppm downfield. The concomitant broadening of these signals may result from the distribution of micelle composition and not from faster exchange with 12-2-12-rich micelles.

(25) (a) Rubingh, D. N. In *Solution Chemistry of Surfactants*; Mittal, K. L., Ed.; Plenum: New York, 1979; Vol. 1, 337. (b) Shinoda, K.; Nomura, T. *J. Phys. Chem.*, 1980, 84, 365. (c) Holland, P. M.; Rubingh, N. D. *J. Phys. Chem.* 1983, 87, 1984.

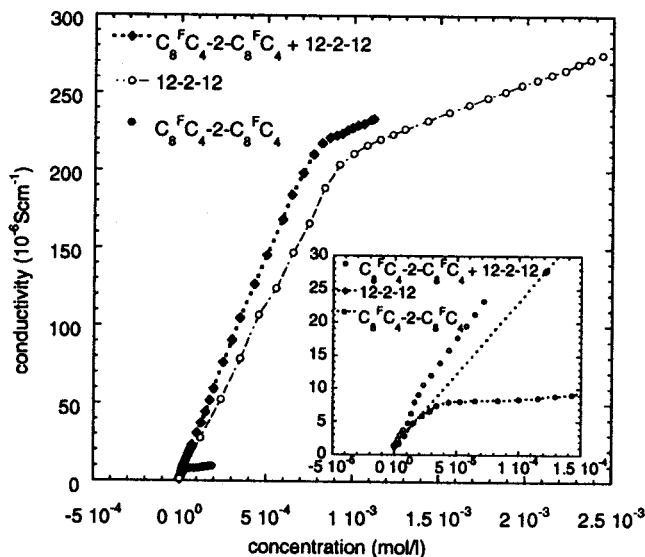


Figure 7. Conductivity, κ , vs concentration curve of an equimolar mixed solution of $C_8^F C_4-2-C_8^F C_4$ and 12-2-12 is plotted along with the conductivity curves of solutions of $C_8^F C_4-2-C_8^F C_4$ alone and of 12-2-12 alone. Note that the horizontal scale is different from that of Figure 1. Here, it represents the concentration of each of the two surfactants in the mixture. The inset is an enlargement of the same curves in the concentration domain of the cmc of $C_8^F C_4-2-C_8^F C_4$.

These mixtures do not show macroscopic phase separation and remain transparent at least up to 50 mM of each surfactant. At 25 °C, the solutions are highly viscoelastic even at concentrations as low as 5 mM. The viscosity decreases as the temperature is increased, and at 65 °C even the 50 mM solution becomes fluid. Cryo-TEM images of a 10 mM solution at 25 °C (of each surfactant) show very long threadlike micelles or narrow ribbons ($>1 \mu\text{m}$). Also many loops and branching are seen (see Figure 10). The loops are 30–100 nm in diameter and may be connected together or connected to short micelle segments.²⁶ Spherical micelles and unilamellar vesicles are seldom found in this mixture, and short micelles are not observed.

(c) Mixing Behavior of Fluorocarbon $C_8^F C_4-2-C_8^F C_4$ and Hybrid Hydrocarbon-Fluorocarbon $C_8^F C_4-2-12$. The conductivity vs concentration curve (Figure 1) shows only one break at $[C_8^F C_4-2-C_8^F C_4] = [C_8^F C_4-2-12] = 26 \mu\text{M}$, indicating mixing of the surfactants. The conductimetry data can be fitted using the regular solution theory (see Appendix), yielding an interaction parameter $\beta = -0.84 \pm 0.46$, again showing an attractive interaction between these two surfactants.

¹⁹F NMR spectra of $C_8^F C_4-2-12$ and $C_8^F C_4-2-C_8^F C_4$ mixed in various proportions yield three sets of signals which can be assigned to the overlapping signals of the two surfactant monomers and to each aggregated surfactant (Figure 9A). The signals of the monomers are at lower field and do not shift with the proportions of the mixture. The signals assigned to aggregated $C_8^F C_4-2-12$ and $C_8^F C_4-2-C_8^F C_4$ are at intermediate and higher fields, respectively, and shift upfield when the mole fraction of $C_8^F C_4-2-C_8^F C_4$ increases. Specifically, the terminal CF_3 signals of $C_8^F C_4-2-C_8^F C_4$ and $C_8^F C_4-2-12$ both shift 0.56

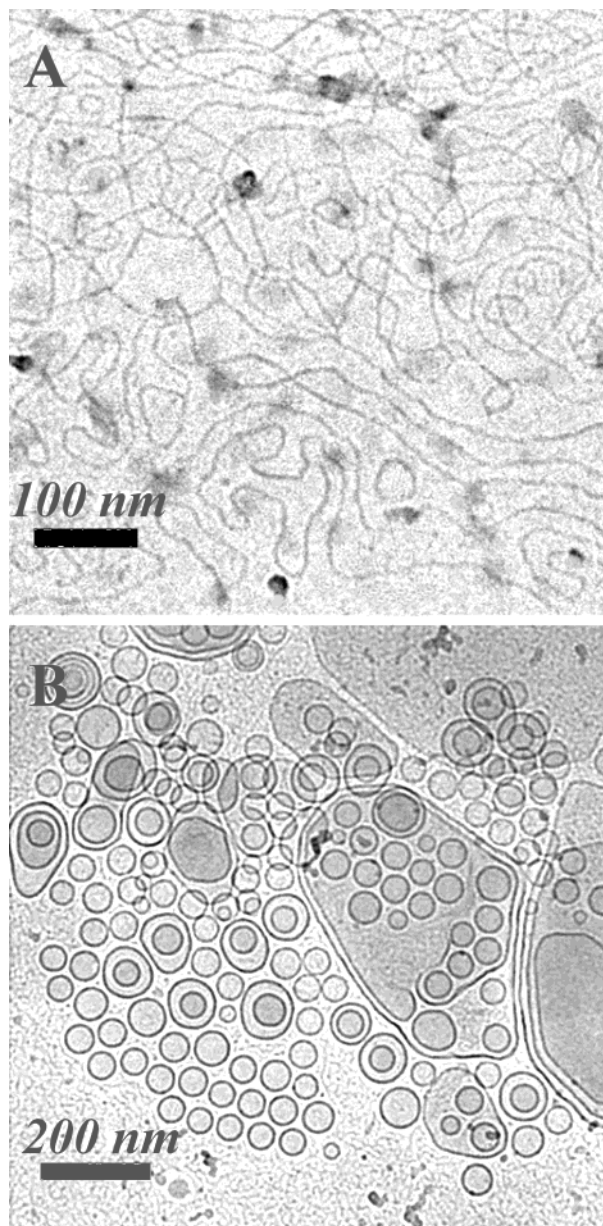


Figure 8. Cryo-TEM images of the upper phase (A) and the lower phase (B) of a $C_8^F C_4-2-C_8^F C_4 + 12-2-12$ mixture at 40 mM each. (A) Highly entangled threadlike micelles are observed, with significant branching and loops. (B) Highly packed unilamellar and multi-lamellar vesicles are observed.

ppm upfield when the mole fraction of $C_8^F C_4-2-C_8^F C_4$ varies from 0.08 to 0.5 (this is in contrast with the downfield shift observed upon addition of 12-2-12 to $C_8^F C_4-2-12$). Considering that these signals are concentration independent in the respective pure surfactant solutions, the shifts apparently reflect directly the changes in polarity within a mixed aggregate when the proportions of hydrocarbon chains and fluorocarbon chains vary. Thus NMR and conductimetry consistently support mixing of those two surfactants.

The 1:1 mixed solutions are slightly opaque, fluid, and monophasic up to 10 mM of each surfactant. Cryo-TEM images show mostly unilamellar vesicles mixed with bilayer sheets (Figure 11). Phase separation occurs above a total concentration of 20 mM. The upper phase is fluid and slightly opaque while the lower phase is more opaque, viscous, and slightly birefringent. Light microscopy observation of this lower phase suggests the presence of

(26) This result is in contrast with a recent observation by Bernheim-Groswasser et al on pure 12-2-12 solution where most loops were connected to networks of micelles, and only a few individual rings were observed (ref 16b).

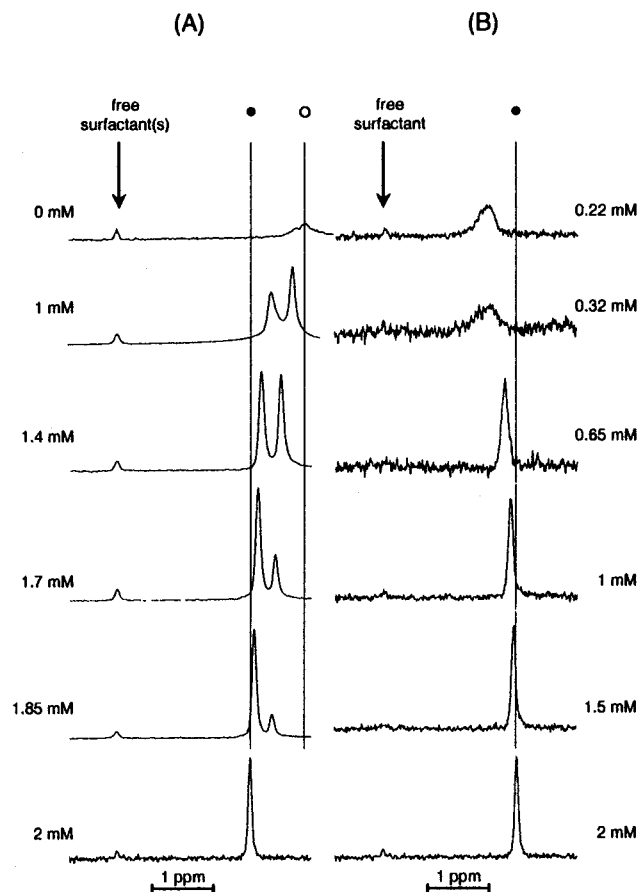


Figure 9. Part of the 400 MHz ^{19}F NMR spectra of mixtures of $\text{C}_8^{\text{F}}\text{C}_4\text{-2-12}$ and $\text{C}_8^{\text{F}}\text{C}_4\text{-2-C}_8^{\text{F}}\text{C}_4$ (A) and of $\text{C}_8^{\text{F}}\text{C}_4\text{-2-12}$ and 12-2-12 (B) in various proportions in 9:1 $\text{H}_2\text{O}/\text{D}_2\text{O}$ (25 °C). For all samples, the total surfactant concentration is 2 mM. The concentration indicated is that of $\text{C}_8^{\text{F}}\text{C}_4\text{-2-12}$. The region contains the signals of the terminal $-\text{CF}_3$ groups in the bulk and in the aggregates. Vertical lines indicate the chemical shift of $\text{C}_8^{\text{F}}\text{C}_4\text{-2-12}$ aggregates (●) and that of $\text{C}_8^{\text{F}}\text{C}_4\text{-2-C}_8^{\text{F}}\text{C}_4$ aggregates (○) alone in solution. Upon mixing $\text{C}_8^{\text{F}}\text{C}_4\text{-2-12}$ with the hydrocarbon 12-2-12 , the ^{19}F signals shift upfield, while they shift downfield upon mixing with $\text{C}_8^{\text{F}}\text{C}_4\text{-2-12}$.

multilamellar vesicles, similar to those observed for pure $\text{C}_8^{\text{F}}\text{C}_4\text{-2-C}_8^{\text{F}}\text{C}_4$ solutions. No threadlike micelles are observed in this system.

Discussion

Critical Micelle Concentrations and Exchange Rates between Surfactants in the Bulk and in the Aggregates. For 12-2-12 , $\text{C}_8^{\text{F}}\text{C}_4\text{-2-12}$, and $\text{C}_8^{\text{F}}\text{C}_4\text{-2-C}_8^{\text{F}}\text{C}_4$, the conductivity increases linearly with concentration with the same slope below the cmc ($2.2 \times 10^5 \mu\text{S}\cdot\text{cm}^{-1}\cdot\text{mol}^{-1}$). This can be understood from the fact that the molar conductivity depends essentially on the ionic part of the molecules, which are the same for the three surfactants.

Critical micelle concentrations of surfactants depend much more directly on the hydrophobic content of the molecules than on their hydrophilic content. Thus, in dimeric surfactants, both the hydrophobic and hydrophilic parts are doubled with respect to the analogue monomeric surfactants, but the cmc's of the dimers are usually orders of magnitude lower than those of the monomers.⁸ Fluorocarbon chains are more hydrophobic than hydrocarbon chains, and for a given carbon chain length, the fluorocarbon surfactant has a lower cmc than the hydrocarbon

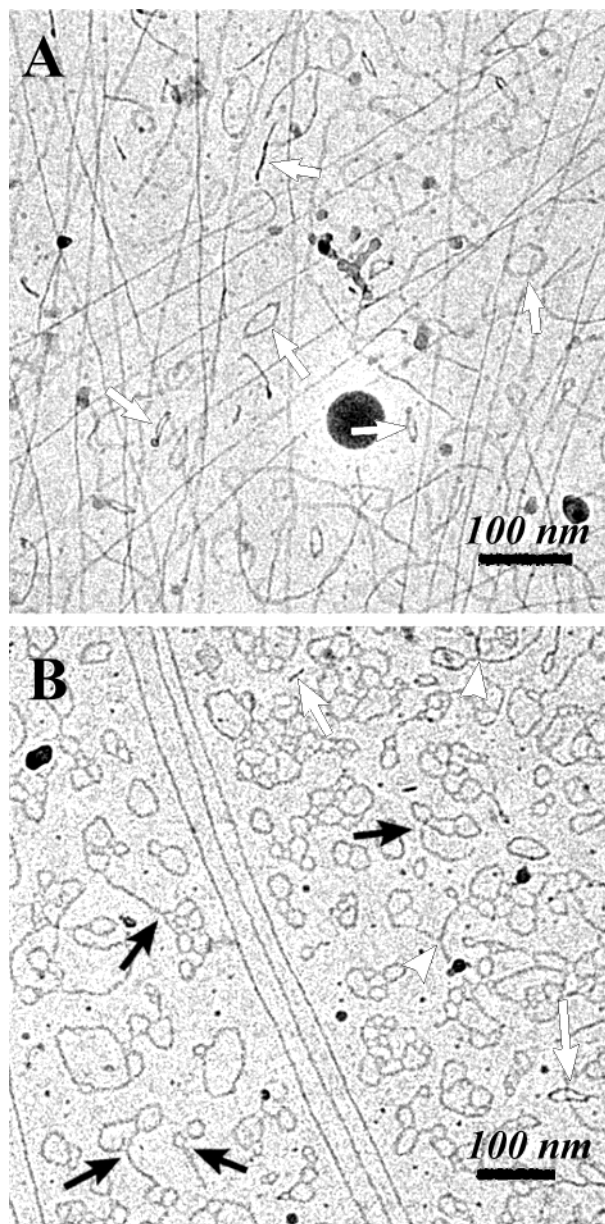


Figure 10. Cryo-TEM image of $\text{C}_8^{\text{F}}\text{C}_4\text{-2-12} + 12\text{-2-12}$ mixture at 10 mM. Very long threadlike micelles and highly branched loops are observed. In some loops, which are seen at different projections, the contrast varies along the circumference (Figure 10A, arrows). Other loops which lie parallel to the film have constant contrast along their circumference. In Figure 10B many individual and connected loops are seen. Some of the loops are connected to other loops, others are connected to short segments of cylindrical micelles (black arrows). Three-fold junctions connecting short segments are also observed (arrowheads).

analogue. An empirical rule states that with respect to the cmc value, a CF_2 unit brings as much hydrophobicity as 1.5 CH_2 units,² although deviation from this rule has been reported for surfactants having hydrocarbon and fluorocarbon segments connected to each other ($-\text{C}_n\text{H}_{2n}\text{C}_m\text{F}_{2m+1}$).²⁷ This rule applies in the case of the fluorocarbon and hybrid hydrocarbon-fluorocarbon surfactants described here. The cmc of $\text{C}_8^{\text{F}}\text{C}_4\text{-2-C}_8^{\text{F}}\text{C}_4$ (28 μM) compares well with that of 16-2-16 (30 μM), and the cmc of $\text{C}_8^{\text{F}}\text{C}_4\text{-2-12}$ (0.2 mM) compares well with that of 16-2-12 (0.14 mM) and 14-2-14 (0.16 mM).

(27) Sadtler, V.; Giuleri, F.; Krafft, M.-P.; Riess, J. G. *Chem. Eur. J.* **1998**, *4*, 1952.

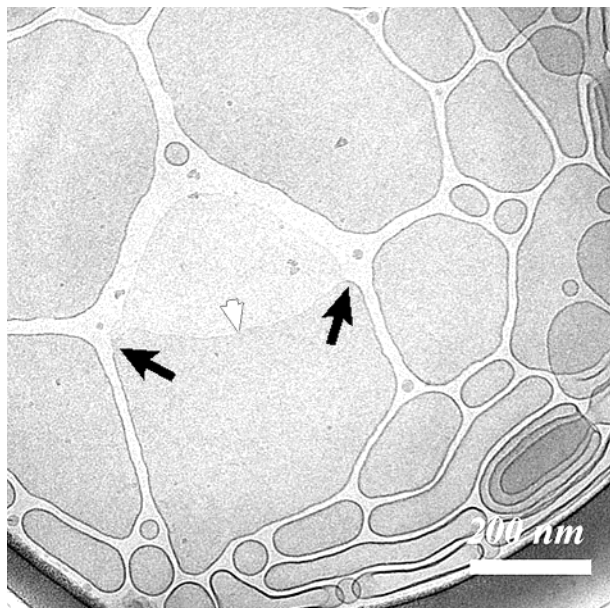


Figure 11. Cryo-TEM image of a $C_8^F C_4-2-12 + C_8^F C_4-2-C_8^F C_4$ mixture at 10 mM. Mostly unilamellar vesicles are observed; no threadlike micelles are observed. Arrows show the boundaries of a broken unilamellar vesicle.

Thus the low cmc's of $C_8^F C_4-2-12$ and $C_8^F C_4-2-C_8^F C_4$ are consistent with the trend followed by $n-2-m$ dimeric surfactants,¹² and with gemini surfactants in general.⁸ However, these results sharply contrast with a recent report by Jouani et al. describing the synthesis of analogous fluorinated dimeric ammonium bromides.²⁸ Those compounds, which have longer alkyl spacers (3–12 carbons) and urea or carbamate moieties connecting the hydrophobic chain to the headgroup, feature unexpectedly high and structure-independent cmc's. For example, surfactants with two $C_8F_{17}C_2H_4-$ chains are reported to have cmc's as high as 100 mM, 4 orders of magnitude higher than the cmc of $C_8^F C_4-2-C_8^F C_4$.

The exchange rate of surfactants between the bulk phase and their aggregates also depends more directly on the hydrophobic content of the molecules than on their hydrophilic content. For $n-2-m$ gemini surfactants, exchange is much slower than that for the analogue monomers.²⁹ When alkyl chains are long enough ($n + m \geq 26$), slow exchange is observed on the NMR time scale, and surfactants in the bulk and in the aggregate are seen as two different sets of signals.¹⁵ The characteristic time of exchange was evaluated at 40 and 100 ms with $n + m = 26$ and $n + m = 28$, respectively.^{15,21} For $C_8^F C_4-2-C_8^F C_4$ and $C_8^F C_4-2-12$, exchange is also slow on the NMR time scale, with the added feature that ¹⁹F NMR is more sensitive than ¹H NMR, yielding a better signal-to-noise ratio at the low concentrations used.

Such slow exchange is highly unusual and was reported only once for a fluorinated surfactant forming hydrogen bonds in the aggregated state.³⁰ Those authors recognized the presence of large aggregates (not micelles) and suggested that this may be of importance in the large values of the measured lifetimes. In our case, the exchange

seems to occur in a similar fashion with spherical and cylindrical micelles or with vesicles. The exchange rate and the concentration of free surfactant simply vary with the hydrophobicity of the molecules, regardless the type of aggregates formed.

On the other hand, slow exchange on the NMR time scale has been reported for numerous other recognition events. These associations often involve the formation of well-defined arrays of coordination bonds to transition metals or hydrogen atoms and large or hindered conformational changes.³¹ To the best of our knowledge, our observations using micelle-forming hydrocarbon cationic amphiphiles, for which no other forces than the hydrophobic effect stabilize the aggregates, are unprecedented.

In the family of surfactants studied here, slow exchange is observed for surfactants with the cmc lower than 0.3 mM. NMR sensitivity, and especially ¹⁹F NMR, allows practical analysis down to 0.01 mM. Similar behavior can be expected for other families of surfactants having large hydrophobic groups and, in particular, among oligomeric surfactants, provided that cmc values are not below the reach of NMR sensitivity.³² Such slow exchange represents a useful tool for the study of micellization and comicellization of surfactants.

Morphology of the Aggregates. The analogy that can be drawn between $C_8^F C_4-2-C_8^F C_4$ and the hydrocarbon 16-2-16 does not extend to the morphology of their aggregates. Despite similar cmc values and of a shared symmetrical structure (two identical hydrophobic chains), their aggregation behaviors are very different. $C_8^F C_4-2-C_8^F C_4$ forms unilamellar vesicles or membranes at low concentration and multilamellar structures with periodicities of ~ 200 nm at higher concentration, while an essential and general feature of the aggregation behavior of the hydrocarbon surfactants $n-2-m$ is to form spherical or spheroidal, micelles at very low concentration, then threadlike micelles at intermediate concentration, and collapsed stacked bilayer structures, often having elongated shapes above a certain concentration (the transition concentration depends on the system).¹² As we have previously reported,¹² those multilamellar stacks observed with the $n-2-m$ hydrocarbon surfactants appear at ca. 40 mM for 14-2-18, 150 mM for 12-2-12, and 320 mM for 8-2-16 and have a periodicity of 4–7 nm, which leaves almost no water between the bilayers.³³ The collapse of the membranes was interpreted as a result of a high charge density at the interface caused by the double positive charge separated only by ~ 3 Å on the gemini headgroup.¹² Apparently, the slight difference in charge density imparted to the larger volume of the fluorocarbon chains suffices to completely modify this behavior, although the headgroups remain the same. Also, the elongated shapes of these stacks (ribbonlike structures), assigned to an ordering of the anisotropic surfactant headgroups within the plane of the bilayer, are not observed for the fluorocarbon bilayers.

(31) See for example Branda, N.; Wyler, R.; Rebek, J., Jr. *Science* **1994**, *263*, 1267; Fujita, M.; Ibukuro, F.; Hagihara, H.; Ogura, K. *Nature* **1994**, *367*, 720.

(32) Lipids, for example, are much more hydrophobic than usual detergents and also exchange slowly between monomeric and vesicular states. However, their critical aggregation concentrations are in the nanomolar range and below, too small for NMR investigations. See: Marsh, D. in *CRC Handbook of Lipid Bilayers*, CRC Press: Boca Raton, **1990**.

(33) Lamellar phases of 12-2-12 swollen with added KBr do not collapse, see ref 10b.

(28) Jouani, M. A.-E.; Szönyi, S.; Dieng, S. Y.; Cambon, A.; Geribaldi, S. *New J. Chem.* **1999**, *23*, 557.

(29) Frindi, M.; Michels, B.; Levy, H.; Zana, R. *Langmuir* **1994**, *10*, 1140.

(30) (a) Fung, B. M.; Mamrosh, D. L.; O'Rear, E. A.; Fresh, C. B.; Afzal, J., *J. Phys. Chem.* **1988**, *92*, 4405. (b) Guo, W.; Brown, T. A.; Fung, B. M., *J. Phys. Chem.* **1991**, *95*, 1829.

Another difference lies in the macroscopic phase separation observed for $C_8^F C_4-2-C_8^F C_4$ above 15 mM, which does not occur with the hydrocarbon gemini surfactants. This is probably due to the higher density of fluorocarbons with respect to hydrocarbons. Finally, all the stacked bilayer structures formed by hydrocarbon $n-2-m$ hydrocarbon surfactants undergo a transition to threadlike micelles upon heating. For 16-2-16, this occurs at 45 °C, and for 18-2-18 this occurs at 60 °C. No such transition was observed for $C_8^F C_4-2-C_8^F C_4$ whose membranes are stable above 70 °C.

In the context of this comparison, the aggregation behavior of the hybrid hydrocarbon-fluorocarbon surfactant $C_8^F C_4-2-12$ becomes particularly interesting, as it bears features of both families. With the hydrocarbon surfactants, $C_8^F C_4-2-12$ shares the capacity to form elongated micelles above its cmc, bilayers at higher concentrations, and also the existence of a transition from bilayers to threadlike micelles upon heating. With the fluorocarbon surfactants, $C_8^F C_4-2-12$ shares the absence of stacked bilayers, the capacity to form vesicles, and the existence of macroscopic phase separations. With respect to the spontaneous curvature of the aggregates, $C_8^F C_4-2-12$ is at an intermediate position between 12-2-12, which forms (long) micelles over a large range of concentrations, and $C_8^F C_4-2-C_8^F C_4$, which exclusively forms bilayers.

Attention should also be paid to the peculiar aggregates formed by $C_8^F C_4-2-12$, where micelles, vesicles, and isolated membranes not only coexist but also clearly transform into one another within the same aggregate (Figure 6). The existence of such connections is very suggestive of the mechanism that can be followed during the transition of a threadlike micelle to a membrane, or vice versa.

Other hybrid hydrocarbon-fluorocarbon surfactants have been described in various contexts such as biomedical applications,³⁴ the formation of multilayered tubules,³⁵ or the study of hydrocarbon and fluorocarbon mixing within micelles,³⁶ vesicles,⁶ or ternary hydrocarbon-fluorocarbon-water emulsions.³⁷ These works and the present study show that a covalent linkage between a hydrocarbon chain and a fluorocarbon chain allows their mixing upon aggregation of the surfactant in water. This contrasts with the usual separation of hydrocarbon and fluorocarbon phases. Whether such a separation or segregation occurs at the molecular level within the aggregates of the hybrid surfactants remains an open question.

From the practical perspective of the excellent oil solubilization properties of dimeric gemini surfactants,³⁸ the hybrid aggregation characteristics of $C_8^F C_4-2-12$ suggest the possibility of mixed detergent properties. This is indirectly answered by the mixing behavior of 12-2-12, $C_8^F C_4-2-12$, and $C_8^F C_4-2-C_8^F C_4$ discussed below.

Mixing Behavior. Hydrocarbons and fluorocarbons are known to have limited mutual miscibility due to the lipophobicity of fluorocarbons. However, phase separation

between hydrocarbon and fluorocarbon surfactants often occurs only partially,³⁹ the formation of two types of aggregates being favored by long hydrophobic moieties.⁴⁰ Many examples of comicellization of hydrocarbon and fluorocarbon surfactants have been reported. In these cases the low miscibility of the surfactants is reflected by a mixed cmc value higher than expected for an ideal mixture. In the regular solution theory,²⁵ the interactions between two types of surfactants in a mixed aggregate are expressed as a parameter β . A repulsive interaction leads to a positive value of β , while $\beta = 0$ expresses ideal mixing and negative β an attractive interaction. Synergistic micellization of hydrocarbon and fluorocarbon surfactants occurs when an attractive force operates, such as the reduction of charge density upon mixing charged and neutral surfactants⁴¹ or charge attraction for oppositely charged surfactants. Most studies on mixed micellar systems have dealt with anionic surfactants, and to the best of our knowledge, the mixing behavior of positively charged hydrocarbon and fluorocarbon surfactants having identical headgroups and hydrophobic chain length has not been investigated.

As shown in the results section, NMR, conductivity and microscopy experiments all indicate that 12-2-12 and $C_8^F C_4-2-C_8^F C_4$ in equimolar proportions segregate almost completely into different assemblies. $C_8^F C_4-2-C_8^F C_4$ forms vesicles and 12-2-12 forms (long) micelles. These aggregates separate macroscopically above 5 mM, presumably because of the different densities of hydrocarbons and fluorocarbons. This low miscibility of hydrocarbon and fluorocarbon cationic gemini likely originates from the high fluorocarbon content (16 CF₂ units) of $C_8^F C_4-2-C_8^F C_4$. Neither the (CH₂)₄ connection between the perfluoroalkyl chain and the headgroups nor the fact that 12-2-12 and $C_8^F C_4-2-C_8^F C_4$ have identical chain length significantly enhances their miscibility.

On the contrary, the hybrid gemini $C_8^F C_4-2-12$ mixes well with both hydrocarbon and fluorocarbon gemini. In both cases, conductimetry shows an attractive interaction (negative values of β). Slow exchange between $C_8^F C_4-2-C_8^F C_4$ and $C_8^F C_4-2-12$ in the bulk and in their aggregates renders comicellization very tractable by NMR. The sensitivity of the ¹⁹F nuclei clearly indicates the changes in polarity upon mixing hydrocarbon and fluorocarbon chains.

Kunitake et al. have previously reported similar mixing between double- and triple-chain amphiphiles bearing one, two, or three hydrocarbon or fluorocarbon chains.⁶ All these amphiphiles assembled into vesicles, and the mixing or demixing occurred between hydrocarbon and fluorocarbon domains within the same vesicle. In the present case, the mixing occurs between surfactants which individually assemble into aggregates of different spontaneous curvatures. The hydrocarbon 12-2-12 has the lower packing parameter and forms elongated micelles at 5 mM. The fluorocarbon $C_8^F C_4-2-C_8^F C_4$ has the higher packing parameter and forms exclusively vesicles at the same concentration. The hybrid surfactant $C_8^F C_4-2-12$ has an intermediate packing parameter and shows bilayers and long micelles coexisting.

Upon mixing, only vesicles or bilayer lamellae and no threadlike micelles are observed in $C_8^F C_4-2-C_8^F C_4 + C_8^F C_4-2-12$ assemblies. However, unlike the vesicles

(34) Myrtil, E.; Zarif, L.; Greiner, J.; Riess, J. G.; Pucci, B.; Pavia, A. A. *Macromol. Chem. Phys.* **1994**, *195*, 1289; Krafft, M.-P.; Riess, J. G. *Biochimie* **1998**, *80*, 489.

(35) Giulieri, F.; Guillo, F.; Greiner, J.; Krafft, M.-P.; Riess, J. G. *Chem. Eur. J.* **1996**, *2*, 1335.

(36) (a) Guo, W.; Li, Z.; Fung, B. M.; O'Rear, E. A.; Harwell, J. H. *J. Phys. Chem.* **1992**, *96*, 6738-6742. (b) Ito, A.; Kamogawa, K.; Sakai, H.; Kondo, Y.; Yoshino, N.; Abe, M. *J. Jpn. Oil. Chem. Soc.* **1996**, *45*, 479.

(37) Yoshino, N.; Hamano, K.; Omiya, Y.; Kondo, Y.; Ito, A.; Abe, M. *Langmuir* **1995**, *11*, 466.

(38) Dam, T.; Engberts, J. B. F. N.; Karthäuser, J.; Karaborn, S.; van Os, N. M. *Colloids Surf. A* **1996**, *118*, 41.

(39) See Stähler, K.; Selb, J.; Barthelemy, P.; Pucci, B.; Candau, F. *Langmuir* **1998**, *14*, 4765 and references therein.

(40) Tamori, K.; Esumi, K. *J. Jpn. Oil. Chem. Soc.* **1992**, *41*, 91.

(41) Funasaki, N.; Hada, S. *J. Coll. Int. Sci.* **1980**, *8*, 376.

formed by $C_8^F C_4-2-C_8^F C_4$ alone, which are stable to heating to 70 °C, the mixed surfactant vesicular solution becomes transparent upon heating suggesting some variation of structure. On the other hand, a 1:1 mixture of $C_8^F C_4-2-12$ and $12-2-12$ consists mostly of very long threadlike micelles with many loops⁴² and branching, and almost no short micelles are observed. Looping and branching decrease the number of micelle terminations (end-caps) without increasing the length of the micelles. Thus, the overall curvature of the aggregates is intermediate between that of $12-2-12$ and that of $C_8^F C_4-2-12$ alone. Besides micelle growth, and direct transition from micelles to ribbons or bilayers, branching and looping represent other ways for the system to adjust to high end-cap energies.

Conclusion

The phase behavior of gemini surfactants with one ($C_8^F C_4-2-12$) or two ($C_8^F C_4-2-C_8^F C_4$) perfluoroalkyl chains was studied and compared to that of analogue hydrocarbon gemini surfactants. The cmc values of the fluorinated gemini surfactants are almost 2 orders of magnitude lower than those of its hydrogenated counterpart. The aggregates formed by the fluorinated surfactants differ strongly from that of the hydrocarbon surfactants. Very stable vesicles have been characterized, along with some peculiar intermediate structures such as threadlike micelles transforming into bilayers or vesicles. In this system, fluorocarbon chains do not simply behave as a more hydrophobic hydrocarbon chain.

These compounds feature slow exchange on the NMR time scale between surfactants in the bulk and surfactants in the aggregates which indicates unusually low characteristic times of exchange for micelle-forming or vesicle-forming cationic surfactants. This slow exchange allows one to easily assess micellization and comicellization of surfactants by NMR.

The respective phase separation of $12-2-12$ and $C_8^F C_4-2-C_8^F C_4$ and coaggregation of $C_8^F C_4-2-12$ with $12-2-12$ and $C_8^F C_4-2-C_8^F C_4$ were characterized. When surfactants with different packing parameters are mixed, it results in aggregates with an intermediate curvature. These systems illustrate several transformations of micellar aggregates leading to the decrease of the overall curvature of the system. Among these transformations are lengthening, branching, and looping of the micelles which all decrease the number of micelle terminations, as well as direct transition of micelles to bilayer structures. Such a variety of structures cannot simply be explained

on the basis of the packing parameter and calls for further work to correlate the surfactant molecular structures and the morphology of their aggregates.

Acknowledgment. This work was supported by Ecole Polytechnique and CNRS. R.O. and I.H. are grateful to S. J. Candau for helpful discussions and to J.-P. Morand for his help with conductivity measurements. The cryo-TEM work was performed at the "Cryo-TEM Hannah and George Krumholz Laboratory for Advanced Microscopy" at the Technion.

Appendix: Nonideality of Surfactant Mixing Behaviors

By use of the regular solution theory,²⁵ the affinity of two different surfactants in micelles can be described by the interaction parameter β .^{39,40} First, the mole fractions of two surfactants in the micelles x_1 and $x_2 = 1 - x_1$ are determined as a function of the mixed cmc value, C_{mixcmc} , and the mole fractions of two surfactants in the solution α_1 and $\alpha_2 = 1 - \alpha_1$, and cmc's of each surfactant, C_1 and C_2

$$x_1^2 \ln[(\alpha_1 C_{\text{mixcmc}})/(x_1 C_1)] = x_2^2 \ln[(\alpha_2 C_{\text{mixcmc}})/(x_2 C_2)] \quad (1)$$

The interaction parameter β can then be written as

$$\beta = \ln[(\alpha_1 C_{\text{mixcmc}})/(x_2 C_2)] x_2^2 \quad (2)$$

Equimolar Mixture of $C_8^F C_4-2-12$ and $12-2-12$. x_1 was calculated by putting the measured cmc values, C_1 (cmc of $C_8^F C_4-2-12$) = 2.2×10^{-4} mol/L, C_2 (cmc of $12-2-12$) = 9.4×10^{-4} mol/L, and $C_{\text{mixcmc}} = 2.89 \times 10^{-4}$ mol/L as well as the mole fractions $\alpha_2 = 1 - \alpha_1 = 0.5$ into the eq 1, and fitting using an in-house Fortran program. The obtained $x_1 = 0.72$ was substituted into the eq 2, and the interaction parameter β was calculated to be -1.24 ± 0.30 .

Equimolar Mixture of $C_8^F C_4-2-C_8^F C_4$ and $12-2-12$. x_1 was calculated by substituting the measured cmc values, C_1 (cmc of $C_8^F C_4-2-12$) = 2.8×10^{-4} mol/L, C_2 (cmc of $C_8^F C_4-2-12$) = 2.2×10^{-4} mol/L, and $C_{\text{mixcmc}} = 2.89 \times 10^{-4}$ mol/L as well as the mole fractions $\alpha_2 = 1 - \alpha_1 = 0.5$ into eq 1, and fitting using an in-house Fortran program. The obtained $x_1 = 0.93$ was substituted into the eq 2, and the interaction parameter β was calculated to be -0.84 ± 0.46 . The calculated value of β is very sensitive to the cmc values which themselves are subject to some errors when the conductivity curves do not show sharp breaks. Error bars of β are calculated by allowing an error of 0.1 mM for the mixed cmc value of $12-2-12 + C_8^F C_4-2-12$ and 0.01 mM for the mixed cmc value of $C_8^F C_4-2-12 + C_8^F C_4-2-C_8^F C_4$.

LA0008075

(42) (a) In, M.; Bec, V.; Aguerre-Chariol, O.; Zana, R. *Langmuir* **2000**, *16*, 141. (b) Danino, D.; Talmon, Y.; Zana, R. *Science* **1995**, *269*, 1420.